

# STUDY ON THE EFFECT OF ADDITIVES ON THE PROPERTIES OF MORTAR USED IN 3D PRINTING TECHNOLOGY WITH A SMALL-DIAMETER NOZZLE

Nguyen Duc Tuan\*, Huynh Phuong Nam, Nguyen Thanh Binh, Nguyen Minh Hai

<sup>1</sup>The University of Danang - University of Science and Technology, Vietnam

\*Corresponding author: ndtuan@dut.udn.vn

(Received: September 07, 2024; Revised: September 27, 2024; Accepted: October 09, 2024)

DOI: 10.31130/ud-jst.2024.534E

**Abstract** - 3D printing in construction simplifies processes by removing formwork, enabling precise automation, and supporting complex structural designs. This study evaluates the effect of admixtures on the properties of mortar used in 3D printing with a nozzle diameter of 5mm. The plasticizing additive Sika Plastiment 96 and the shrinkage-reducing admixture Sika Intraplast Z-HV, at varying dosages, were employed to design 20 mortar mix trials. A series of experiments were conducted to assess the flowability, retention of flowability, load-bearing capacity of printed layers, and mechanical strength of the mortar. The results indicate that the dosage of admixtures significantly affects the printability and compressive-flexural strength of the hardened mortar. The optimal admixture ratio of Intraplast Z-HV and Plastiment-96 was determined to be 0.6:0.45%, the designed mortar mix retained printability for up to 40 minutes with a 5mm nozzle, and the maximum number of layers printable in one session was 20.

**Key words** - 3D printing mortar; plasticizing additive; shrinkage-reducing additive; printability; load-bearing capacity of printed layers.

## 1. Introduction

In recent years, construction technology using 3D printing methods has been making groundbreaking advancements [1], this has been demonstrated through numerous real-world projects featuring complex geometries that are fully 3D-printed in an automated process with high precision and excellent aesthetics [2, 3]. In addition, with the rapid development of Building Information Modeling (BIM) in recent years, 3D printing technology is increasingly expected to automate and address construction challenges such as shortening timelines, eliminating the need for formwork, and enhancing the precision of complex structural details based on available BIM models [4]. However, for 3D printing technology to be more widely adopted in the near future, alongside the development of mechanical systems and software integration to automate the printing process, optimizing the composition of the print material, such as concrete or mortar, to meet the technical requirements of 3D printing is a critically important area of research.

Currently, many studies are focusing on analyzing the effects of mixed composition on certain fundamental properties of concrete or mortar when applied to 3D printing technology [5-6]. Research shows that the material mixture must have adequate flowability to be continuously supplied to the nozzle without clogging, while simultaneously possessing the ability to retain its shape according to the design structure after extrusion [7]. If the material mixture has excessively low flowability, it will

cause nozzle clogging. Conversely, if the material is too fluid, it will lose its ability to maintain shape after exiting the nozzle. The requirements for this property also vary depending on the use of nozzles with different diameters. Utilizing smaller nozzles can facilitate the construction of components that require high levels of detail. However, there are few studies worldwide focusing on nozzle diameters below 10 mm [8-9]. Reducing the nozzle diameter increases the risk of clogging, which presents a significant challenge when decreasing the diameter of the printing nozzle. To address this issue, the print mixture needs to have higher flowability. Additionally, mortar mixtures are considered more feasible than conventional concrete, as the larger aggregates in concrete can cause blockages in the piping during pumping and extrusion.

Moreover, the bond strength between layers will decrease with the time interval between printing passes [16]. Therefore, reducing the time interval between the printing of two layers not only helps increase the printing speed but also enhances the bond between the printed layers, thereby improving the quality of the structure. However, if the layers are stacked too early before the previous layer has achieved an appropriate strength level, it may cause deformation or damage to the previously printed layers. Thus, it is essential to evaluate the shape stability and load-bearing capacity of the material layer over a specific time period after printing. Lastly, phenomena such as clogging, localized hardening, and shrinkage of the mixture can contribute to the occurrence of cracks in structures when applying 3D printing technology. Therefore, these characteristics also need to be appropriately assessed when developing the material mixture.

For the aforementioned properties, in addition to optimizing the amounts of cement, water, and aggregates in mortar or concrete, the rational use of admixtures is a necessary approach. Numerous studies worldwide have investigated the use of admixtures to modify the properties of concrete to make it suitable for 3D printing processes. These studies typically focus on the effects of mineral and chemical admixtures on the coagulation process of fine particles or on enhancing the hydration of cement through physicochemical mechanisms, which help improve flow properties and accelerate the strength development of the mortar [11-14]. These types of admixtures typically focus on accelerating the early strength development but can also lead to a rapid decrease in flowability, necessitating the use

of specialized equipment to mix the mixture directly at the print head. To address this issue, the combination of plasticizers and expanding agents has been considered as a novel approach. This combination not only helps improve strength but also maintains the flowability of the mixture, minimizes shrinkage, and thus reduces the occurrence of cracks in the 3D-printed mortar product. Additionally, it addresses the limitations of previously used admixtures. However, the effects of the dosage and types of these admixtures on the fundamental properties of the mortar mixture when applied in 3D printing technology have not yet been clarified in previous studies.

Therefore, this study aims to clarify the influence of the type and dosage of admixtures on the printability of the mortar mixture used in 3D printing technology with a small nozzle diameter of only 5 mm. The plasticizer Sika Plastiment 96 and the shrinkage-reducing agent Sika Intraplast Z-HV at varying dosages were utilized to design experiments for 20 different mix compositions of the mortar. A series of experiments were conducted to determine the flowability, flow retention, load-bearing capacity of the printed layers, as well as the mechanical strength of the mortar after curing. The experimental results were analyzed to derive general trends regarding the impact of each admixture dosage on printability-related properties and to propose the optimal mix composition for the case of using a 5 mm nozzle.

## 2. Materials and Experimental Methods

### 2.1. Materials Used

In cases where the 3D printing nozzle is smaller than 5mm, the use of aggregates such as crushed stone or coarse sand, as in conventional concrete, can lead to blockages, making the use of fine aggregates a more suitable approach. Additionally, a portion of the cement should be replaced with fly ash or silica fume (SF) to improve pumpability and extrudability, enhancing the thixotropic properties of the concrete mix. Chemical admixtures and rheology modifiers also need to be employed depending on the specific application of the mixture [15, 16]. Based on the initial analysis, the mortar mixture used in the study includes cement, water, silica fume mineral admixture, fine aggregates, and various plasticizing and shrinkage-reducing additives.

Specifically, the cement used is Hai Van Portland Cement PC40 with a specific gravity of 3.02 g/cm<sup>3</sup> and a 28-day compressive strength of 43.0 N/mm<sup>2</sup>. The aggregate is finely ground limestone powder, originating from Đại Hiệp quarry, Quảng Nam Province, Vietnam. The fine aggregate (FiA) has a specific gravity of 2.76 g/cm<sup>3</sup> and a loose bulk density of 1024 kg/m<sup>3</sup>. The active mineral admixture used is silica fume (SF), supplied by Sika in 25kg bags, with a recommended dosage of 5-10%, and its physical and mechanical properties meet the requirements of TCVN 8827:2011.

The plasticizing additive Sika Plastiment-96 (P96) used in the study is a lignosulfonate-based admixture, compliant with ASTM C494 Type D. It has a specific gravity of 1.16-1.18 kg/l, and its function is to delay setting time without

slowing down the hardening process, while also enhancing strength after curing. Another additive incorporated is the shrinkage-reducing additive Sika Intraplast Z-HV (IZ), which is in powder form with a specific gravity of 1.05 kg/l. This additive reduces volume expansion during application and improves the workability of the mortar mix without causing segregation or bleeding, thereby enhancing the bond between the layers of mortar during the 3D printing process.

### 2.2. Mix Design

To clarify the influence of additives on the fundamental properties of the mortar mix, the study conducted an experimental design with 20 different mix proportions, as presented in Table 1. The amounts of cement, silica fume, and limestone powder were fixed across all mixes. The independent variables considered in the study were the dosage of the plasticizing additive Sika Plastiment-96 (P96) and the content of the shrinkage-reducing additive Sika Intraplast Z-HV (IZ). Specifically, the mass ratio of the IZ additive varied from 0.5% to 0.8%, while the dosage of the P96 additive was changed from 0.35% to 0.55%. Additionally, there were slight variations in water content among the different mixes to optimize workability, ensuring that the mortar mixes met the requirements for printing with a nozzle diameter of 5 mm in the initial phase. This is a prerequisite for determining the printability of the mortar mix before proceeding with subsequent tests in the study.

**Table 1.** Mix Proportions Used

Mix No. (CP)	IZ	P96	W/C	C	FiA	W	SF	IZ	P96
	%	%		kg	kg	lit	kg	kg	l
1.1	0.5	0.35	0.522	735.6	799.6	384.0	64.0	4.0	2.57
1.2		0.40	0.521	735.6	799.6	383.2	64.0	4.0	2.94
1.3		0.45	0.520	735.6	799.6	382.5	64.0	4.0	3.31
1.4		0.50	0.519	735.6	799.6	381.8	64.0	4.0	3.68
1.5*		0.55	0.518	735.6	799.6	381.0	64.0	4.0	4.05
2.1	0.6	0.35	0.517	735.6	799.6	380.3	64.0	4.8	2.57
2.2		0.40	0.516	735.6	799.6	379.6	64.0	4.8	2.94
2.3		0.45	0.515	735.6	799.6	378.8	64.0	4.8	3.31
2.4		0.50	0.514	735.6	799.6	378.1	64.0	4.8	3.68
2.5*		0.55	0.513	735.6	799.6	377.4	64.0	4.8	4.05
3.1	0.7	0.35	0.514	735.6	799.6	378.1	64.0	5.6	2.57
3.2		0.40	0.513	735.6	799.6	377.4	64.0	5.6	2.94
3.3		0.45	0.512	735.6	799.6	376.6	64.0	5.6	3.31
3.4		0.50	0.511	735.6	799.6	375.9	64.0	5.6	3.68
3.5*		0.55	0.51	735.6	799.6	375.2	64.0	5.6	4.05
4.1	0.8	0.35	0.511	735.6	799.6	375.9	64.0	6.4	2.57
4.2		0.40	0.509	735.6	799.6	374.4	64.0	6.4	2.94
4.3		0.45	0.507	735.6	799.6	372.9	64.0	6.4	3.31
4.4		0.50	0.505	735.6	799.6	371.5	64.0	6.4	3.68
4.5*		0.55	0.503	735.6	799.6	370.0	64.0	6.4	4.05

### 2.3. Experimental Methodology

The study focuses on evaluating the properties related to printability, which includes: (i) workability and the ability to maintain workability, (ii) load-bearing capacity of the printed layers, and (iii) compressive and flexural strength of the mortar after curing.

Currently, there is no standardized method for evaluating the workability of concrete and mortars used in 3D printing. Therefore, the study conducted preliminary

testing using four methods, including the workability test of concrete mixtures using a manual flow table slump test, the workability test of concrete mixtures using a Suttard viscometer, and the standard consistency test of cement paste using a Vica  $\phi 10$  device [17-19]. The test results for some of the mixtures in Table 1 according to these methods are presented in Table 2.

**Table 2.** Results of Workability Testing Using Different Methods.

Mix No. (CP)	Manual flow table	Suttard viscometer	Vica $\phi 10$
	$D_{TB}$ (mm)	$D_{TB}$ (mm)	mm
1.1	126.0	5	2
1.5	134.5	5	4
2.1	130.0	5	4
2.5	134.5	5	5
3.1	131.0	5	4
3.5	138.5	5	1
4.1	132.0	5	5
4.5	137.0	5	0
Deviation	12	0	3

Table 2 shows that the Suttard viscometer method could not be applied due to the lack of significant differences between the various mixtures. The slump test and Vica method demonstrated clear differences between the mixtures, allowing for an assessment of the impact of compositional changes on the workability of the mortar mixture. However, the slump test only determines the workability of the mixture at a specific moment, making it challenging to assess the duration of workability. In contrast, the Vica method allows for multiple tests to collect time-related differences in the mortar mixture, thereby determining the time frame during which the mixture can maintain its plasticity during printing. Therefore, the study selected the Vica needle method to evaluate the workability and the ability to maintain workability of the mortar mixture, as shown in Figure 1a [19]. Specifically, the study used a Vica needle with a diameter of 5 mm and conducted repeated experiments every 5 minutes. The distance from the bottom of the sample to the tip of the Vica needle is defined as the penetration resistance (mm), a larger value indicates lower plasticity of the mortar mixture, and vice versa. Additionally, for each mixture, a trial printing experiment using a nozzle with a diameter of 5 mm was conducted, as shown in Figure 1(b), to clarify the relationship between the results of the Vica needle test and the actual printing ability. Experiments on the baseline mixture demonstrated that when the penetration resistance measured with the Vica needle Vica  $\phi 5$  exceeds 5 mm, the mortar mixture cannot flow through the nozzle with a diameter of 5 mm.

On the other hand, to evaluate the ability to support printed layers, experiments using a real nozzle were conducted to replicate the loading effects of the printed strands on the first printed layer. This allowed for the observation of the extent of height reduction of the printed layer and the shape retention of the sample after being subjected to loading, as shown on the left side of Figure 2. Additionally, to facilitate the measurement of the slump of the mortar over time, three cylindrical samples with a

diameter of 50 mm were used for each mixture, as shown on the right side of Figure 2. Initially, the mortar mixture was poured into a plastic mold with a height of 50 mm. After 5 minutes, the plastic tube was removed from the mortar mixture. Subsequently, a flat plastic sheet was placed on top of the mortar sample, and loading was applied for the next layer every 5 minutes. The loading material used in this process was sand, with the mass of each sand layer equivalent to the mass of the initial mortar sample. This procedure was conducted for three cycles for each sample. The load in each cycle was calculated to match the load of each printed layer. The height of the mortar sample was measured after each loading cycle.



(a) Vica needle test

(b) Test printing experiment

**Figure 1.** Workability test and ability to support printed layers

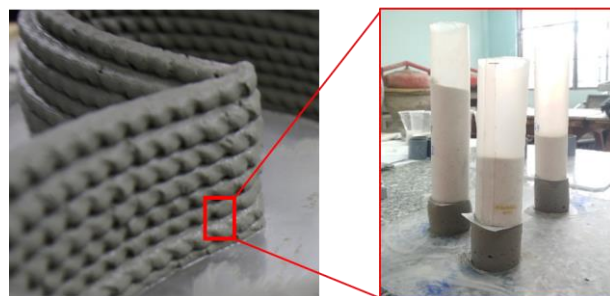


**Figure 2.** Experiment on the load-bearing capacity of the printed layer above.

Finally, the compressive and flexural strength tests for the 20 mixtures were conducted according to TCVN 3121-11 [18]. Since this study focuses primarily on workability and printability, the mechanical strength tests were performed at 3 days of age for all concrete mixtures.

### 3. Results and Discussion

#### 3.1. Influence of Additives on Workability and Retention of Workability of Mortar Mixtures

Table 3 presents the results of the Vica needle test with a diameter of 10 mm and its correlation with the printing capability using a 5 mm diameter nozzle. The results indicate that when the penetration depth measured by the Vica needle is less than 2.0 mm, the mortar mixture exhibits excessive plasticity and lacks the ability to maintain shape during the printing process. Conversely, for mixtures with an initial penetration depth of 5.0 mm, the mortar can flow smoothly through the nozzle without causing blockages. Therefore, a penetration depth greater than 2.0 mm for the Vica needle is considered an appropriate range for the mortar mixture to ensure adequate printing capability at the initial stage.

**Table 3.** Results of Vica Needle Testing and 3D Printer Testing

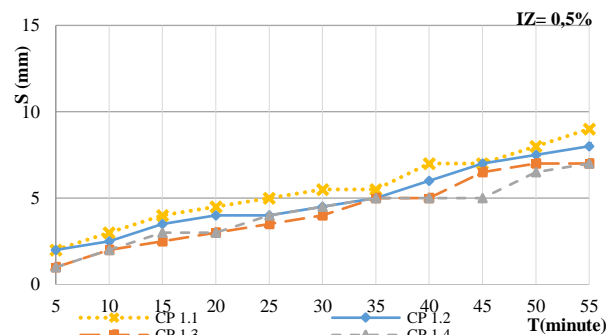
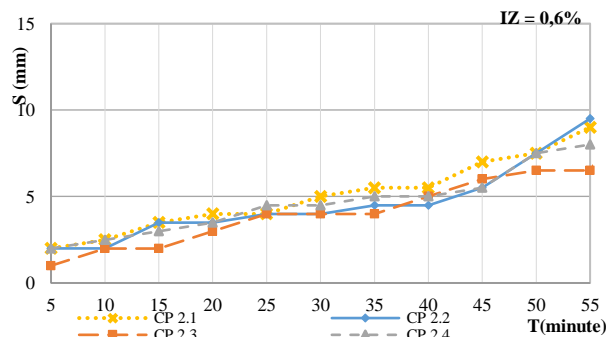
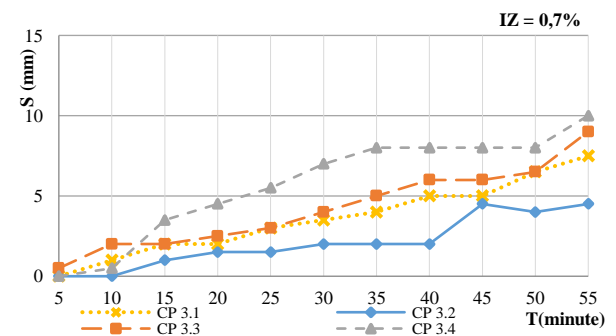
Mix No (CP)	1.1	1.2	1.3	1.4	1.5	2.1	2.2	2.3	2.4	2.5
Penetration resistance (mm)	2.0	5.0	4.0	4.0	4.0	4.0	3.5	3.5	5.0	5.0
3D Printer Testing	Good	Good	Good	Good	Good	Good	Good	Good	Good	Good
Mix No (CP)	3.1	3.2	3.3	3.4	3.5	4.1	4.2	4.3	4.4	4.5
Penetration resistance (mm)	4.0	2.5	2.0	2.0	1.0	5.0	2.0	3.0	2.0	0.0
3D Printer Testing	Good	Good	Good	Good	Loose	Good	Good	Good	Good	Loose

To assess the workability retention of the mortar mixtures, tests were conducted using a Vica needle with a diameter of 5 mm, as described in section 2. Results presented in Figures 3(a) to 3(d) illustrate the relationship between time and penetration resistance  $S$  (mm) for mortar mixtures with IZ content ranging from 0.5% to 0.8%. Here, the mortar mixture is considered to maintain its initial printability when the penetration resistance falls within the range of 0 to 5.0 mm. Figure 3 shows that the penetration resistance increases over time due to the hardening process of the mortar mixture. Generally, all mortar mixtures retain their printability within the time range of 35 to 45 minutes, meaning the penetration resistance during this period remains within 0 to 5.0 mm. In Figures 3(b) and 3(c), the IZ ratios of 0.6% to 0.7% help the mortar mixtures maintain penetration resistance below 5 mm for a longer duration compared to the mixtures with IZ ratios of 0.5% and 0.8%. However, after the 40-minute mark, the rate of workability loss of the mixtures increases rapidly, and by the 55-minute mark, most of the tested mixtures exhibit penetration resistance nearing 10 mm. This can be understood as the hydration reaction begins to occur strongly during this time, forming a C-S-H gel that forms a network that binds cement and sand particles together. The formation of C-S-H gel is the primary reason for the accelerated loss of workability in the mortar [20-21].

With the variation in P96 dosage at different levels, there is a significant impact on the initial mixing water content. An increase in P96 dosage reduces the free water during mixing, thereby increasing the workability of the mortar mixture. Thus, to ensure that the mixtures have similar initial consistency and workability, the water-to-cement (W/C) ratio needs to be reduced as the P96 dosage increases. This adjustment ensures the initial consistency of the mortar, achieving a Vica needle penetration of  $\phi 10$  within the range of 2 to 5 mm. The simultaneous increase in P96 and reduction in the W/C ratio make the change in Vica needle penetration resistance not particularly noticeable. However, when using P96 within the range of 0.35% to 0.50%, all mixtures demonstrated an extended period of maintaining printability. Notably, the mixtures with P96 dosages of 0.40% and 0.45% exhibited better performance in prolonging the workability period compared to the other mixtures.

On the other hand, using a low IZ content of 0.5%, as shown in Figure 3(a), only maintains printability for about 35 minutes. In contrast, Figure 3(b) indicates that mixtures with higher P96 and IZ content tend to sustain lower penetration resistance for up to 40 minutes and even up to 45 minutes. Despite reducing the W/C ratio in the mixtures

of Figure 3(c) compared to those in Figure 3(b) as a result of increasing IZ and P96, the W/C ratio seems to affect the initial plasticity but is not the key factor in extending the workability retention time. Increasing the IZ content to 0.8%, as shown in Figure 3(d), reduces the printability retention time to below 35 minutes. This is due to IZ's mechanism of creating small air bubbles in the wet mix, which expands the volume of the mortar before setting. These micro-bubbles allow the aggregates to slide more easily, improving workability and plasticity, but too many bubbles can reduce the mixture's flowability. Therefore, the optimal P96 content is between 0.4-0.45%, and the optimal IZ content is between 0.6-0.7%. Mixtures using additives in these ranges can maintain printability for up to 40 minutes. The mixture with the longest printability retention time,  $T = 45$  minutes, corresponds to CP 3.2 with IZ and P96 ratios of 0.7% and 0.40%, respectively.

**Figure 3(a).** Graph showing the effect of P96 ratio on workability retention time when IZ = 0.5%**Figure 3(b).** Graph showing the effect of P96 ratio on workability retention time when IZ = 0.6%**Figure 3(c).** Graph showing the effect of P96 ratio on workability retention time when IZ = 0.7%

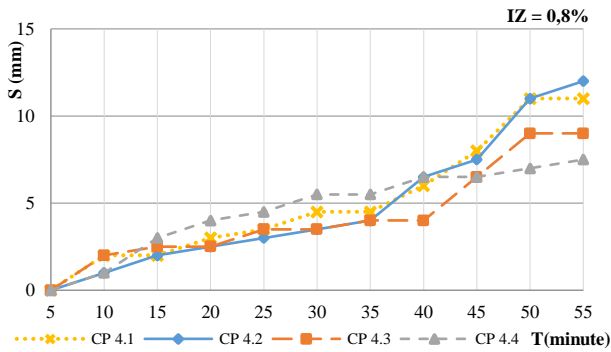


Figure 3(d). Graph showing the effect of P96 ratio on workability retention time when  $IZ = 0.8\%$

### 3.2. Influence of Additives on the Load-Bearing Capacity of the Printed Layers

Figures 4(a) to 4(d) illustrate the ratio of the sample height after being subjected to the load from the upper layers compared to the initial sample height, corresponding to the use of IZ additive in the range of 0.5% to 0.8%, based on the experimental procedure outlined in section 2.3. The load-bearing capacity of the printed layers is higher when the height of the mortar sample after loading remains close to the initial height. Figure 4 shows a clear trend of height reduction as the number of load layers increases. However, the degree of reduction varies between different mixture compositions. In Figure 4(a), with an IZ ratio of 0.5%, the reduction in sample height is almost linear for all four tested mixtures. In Figures 4(b) to 4(d), it can be seen that the reduction in height is fastest for the first layer. The second layer holds its shape better, while the height reduction in the third layer varies depending on the P96 ratio. For the third printed layer, mixtures with IZ ratios between 0.6% and 0.7% show significantly less reduction compared to those with IZ ratios of 0.5% and 0.8%. This behavior can be explained by the fact that IZ is an expanding additive. In the 5 to 10 minutes after mixing, the expansion reaction generates small air bubbles, which help reduce the height loss when subsequent layers are loaded. However, if a higher amount of IZ is used, the excessive generation of air bubbles can decrease the load-bearing capacity of the next printed layers.

On the other hand, Figure 4 shows that mixtures with P96 ratios ranging from 0.45% to 0.5% exhibit better load-bearing capacity for the printed layers compared to other mixtures. The use of an increased P96 additive ratio corresponds to a reduction in the W/C ratio. When the P96 additive ratio increases and the W/C ratio decreases, the mortar mixture may lose its workability more quickly, thereby demonstrating improved load-bearing capacity for the printed layers compared to other mixtures. With a P96 additive ratio of 0.45% to 0.5% and an IZ shrinkage-reducing additive ratio of 0.6% to 0.7%, the mixtures using these additive levels show superior capacity to maintain load-bearing strength for the printed layers. Mixture CP 2.3 ( $IZ, P96 = (0.6\%, 0.45\%)$ ) has the lowest height reduction under load, with 98.88% remaining after one load layer, 97.45% after two load layers, and 95.13% remaining after three load layers.

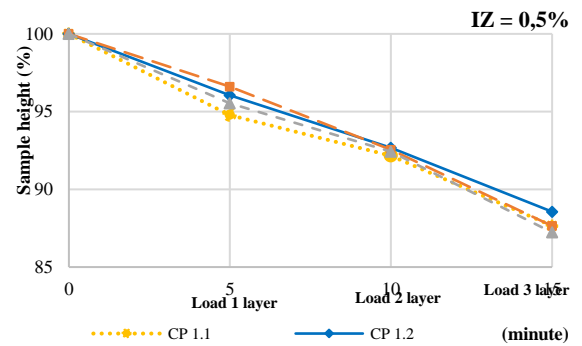


Figure 4(a). Graph showing the effect of the P96 ratio and the W/C ratio on the load-bearing capacity of the top print layer when the  $IZ = 0.5\%$

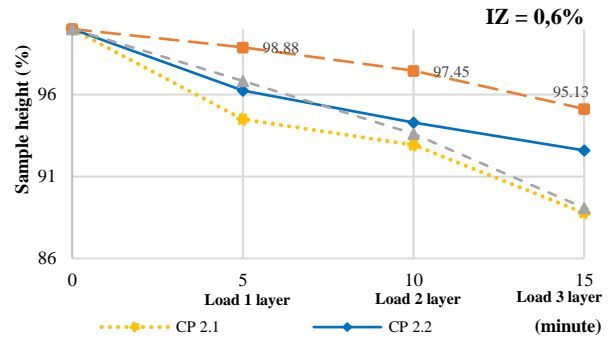


Figure 4(b). Graph showing the effect of the P96 ratio and the W/C ratio on the load-bearing capacity of the top print layer when the  $IZ = 0.6\%$

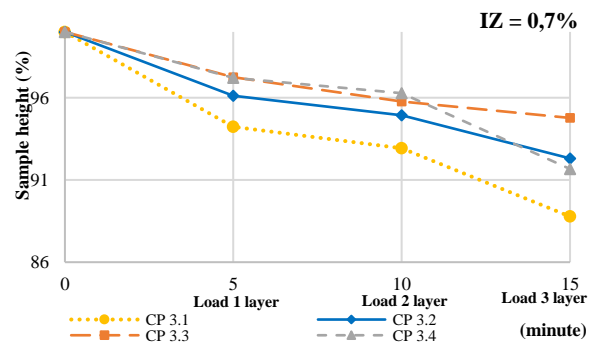


Figure 4(c). Graph showing the effect of the P96 ratio and the W/C ratio on the load-bearing capacity of the top print layer when the  $IZ = 0.7\%$

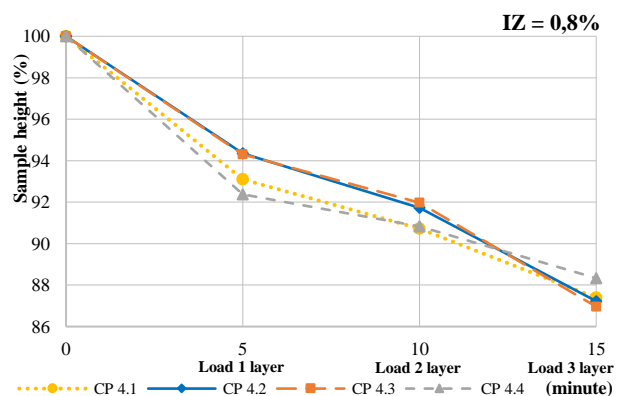


Figure 4(d). Graph showing the effect of the P96 ratio and the W/C ratio on the load-bearing capacity of the top print layer when the  $IZ = 0.8\%$



### 3.3. Effect of Additives on the Flexural and Compressive Strength of Mortar

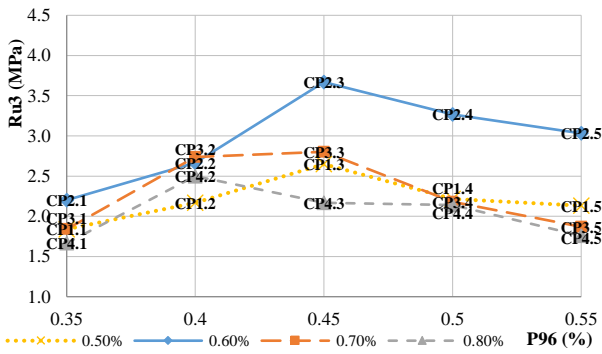


Figure 5(a). Graph illustrating the effect of Plastiment-96 ratio on  $Ru^3$  corresponding to the ratios of IZ = 0.5%, 0.6%, 0.7%, 0.8%

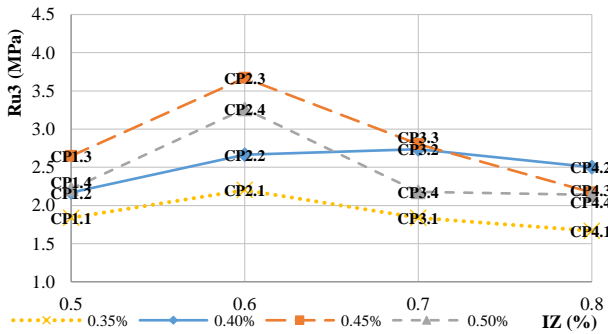


Figure 5(b). Graph illustrating the effect of Intraplast Z-HV ratio on  $Ru^3$  corresponding to the ratios of P96=0.35%, 0.40%, 0.45%, 0.50%

The effect of additives on compressive strength is illustrated in the following graphs.

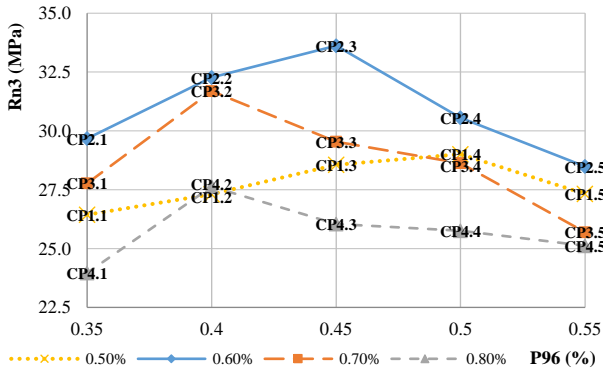


Figure 6(a). Graph showing the effect of the Plastiment-96 ratio on  $Rn^3$  corresponding to the ratios of IZ = 0.5%, 0.6%, 0.7%, 0.8%

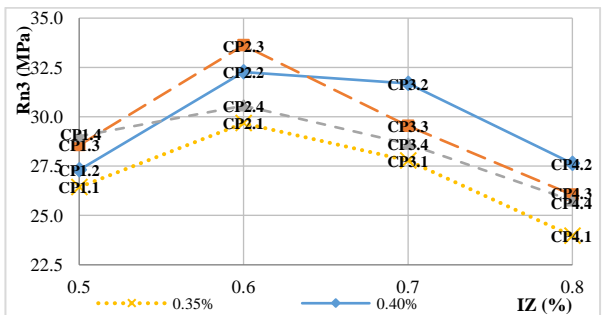


Figure 6(b). Graph showing the effect of the Intraplast Z-HV ratio on  $Rn^3$  corresponding to the ratios of P96=0.35%, 0.40%, 0.45%, 0.50%

The experimental results regarding the flexural strength of mortar samples after 3 days of curing are presented in Figures 5(a) and 5(b), while the compressive strength results for the same curing age are shown in Figures 6(a) and 6(b). Overall, there is a high correlation between the flexural and compressive strength test results. In other words, samples with high flexural strength also exhibit high compressive strength, and vice versa. In all figures, maintaining a constant IZ ratio while increasing the P96 ratio leads to an increase in both flexural and compressive strength due to the water-reducing effects of the plasticizing additive. A P96 ratio of 0.45% yields the best results for both flexural and compressive strengths. However, when the dosage of P96 exceeds 0.45%, strength tends to plateau or even decrease. This phenomenon may occur because using a plasticizing additive in excessive amounts can result in segregation and excess water within the mortar mixture, prolonging the setting and hardening times of the mortar. Consequently, this leads to slower strength development and lower ultimate strength than expected. Another important factor to consider is that the cement content in the mortar mixtures in this study exceeds 700 kg/m<sup>3</sup>, significantly higher than that in conventional mortar mixes. Since the ratio of additives is calculated based on the mass of cement, the amount of additive used per cubic meter of mortar also increases substantially, resulting in potential overdosing of the plasticizing agent, despite the usage ratio being only 0.45%. Additionally, the simultaneous use of two types of additives can accelerate the occurrence of overdosing.

When maintaining a constant P96 ratio and increasing the IZ ratio, the strength tends to increase and reaches its peak at an IZ ratio of 0.6%, after which it gradually decreases. The effect of IZ is to reduce water separation and create air bubbles in the mortar mixture before setting. Therefore, when used in moderate amounts, it helps reduce the free water during mixing, thereby increasing the strength of the mortar, while a uniform distribution of fine air bubbles will not compromise the strength of the mortar. However, when used in excessive quantities, the air bubbles may become larger and more numerous, leading to a decrease in both flexural and compressive strength. The optimal combination ratio of the two additives, IZ and P96, resulted in maximum values of flexural strength ( $Ru^3$ ) of 3.67 MPa and compressive strength ( $Rn^3$ ) of 33.62 MPa, exceeding 30 MPa at the mix ratio CP 2.3 (IZ, P96) = (0.6%, 0.45%).

### 3.4. Results of the Printing Experiment Using a 5mm Nozzle for the Optimal Mixture

Based on the experiments regarding the maintenance of printability, load-bearing capacity of printed layers, and considering both flexural and compressive strengths, the research group selected the optimal printing mixture CP 2.3 (IZ, P96) = (0.6%, 0.45%) for use in a 3D printer with a 5mm nozzle. The actual printed product is shown in Figure 7. The printing process demonstrated that even after 40 minutes of printing, the mixture continued to meet the printing requirements. More than 20 layers were printed, and in terms of aesthetics and geometry, the mixture still met the necessary standards.

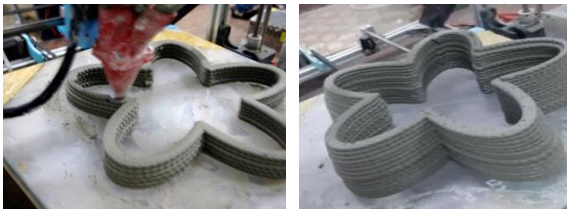


Figure 7. 3D-printed mortar sample of CP 2.3

#### 4. Conclusion

This study focuses on designing a 3D printing mortar mix for a nozzle diameter of 5 mm, utilizing a binder-to-aggregate ratio of 1:1, incorporating ultra-fine aggregates, silica fume, chemical additives, and shrinkage-reducing agents. The independent variables include the dosage of plasticizing additives and the content of shrinkage-reducing additives, optimized to achieve properties such as printability, maintenance of printability over time, shape stability, and mechanical strength. Key findings from the research are as follows:

i. For a nozzle diameter of 5 mm, the mortar mix exhibits printability when the penetration resistance measured by the Vica needle  $\phi$  10 is greater than 2.0 mm. A penetration resistance of less than 2.0 mm renders the mortar mix overly plastic and unable to maintain its shape, while a penetration resistance greater than 5.0 mm using the Vica needle  $\phi$  5 results in clogging at the nozzle.

ii. The optimal dosage of the plasticizer P96 is in the range of 0.4 – 0.45%, while the suitable dosage of the shrinkage-reducing additive IZ is 0.6 – 0.7%. Mixtures using these dosages can maintain printability for up to 40 minutes. The formulation with the longest printability duration is  $T = 45$  minutes, corresponding to the mix design CP 3.2 (IZ, P96) = (0.7%, 0.40%).

iii. With the plasticizer P96 dosage ranging from 0.45 to 0.5% and the shrinkage-reducing additive IZ at 0.6 to 0.7%, the mixtures using these dosages demonstrate better load-bearing capacity for the printed layers. The mix design CP 2.3 (IZ, P96) = (0.6%, 0.45%) exhibited the least height reduction under load, with a remaining height of 98.88% after one load layer, 97.45% after two load layers, and 95.13% after three load layers.

iv. The combined ratio of the two additives Intraplast Z-HV and Plastiment-96 resulted in the highest values for both bending strength ( $R_u$ ) and compressive strength ( $R_n$ ), with  $R_{u3} = 3.67$  MPa and  $R_{n3} = 33.62$  MPa, exceeding 30 MPa at the mix design CP 2.3 (IZ, P96) = (0.6%, 0.45%).

v. The 3D printing trial using a 5.0 mm nozzle with the optimal mix design from point iv demonstrated that after 40 minutes of printing, the mixture still met the printing requirements. The number of printed layers reached over 20, and in terms of aesthetics and geometry, the mix design continued to meet the standards.

**Acknowledgments:** This research is funded by The University of Danang – University of Science and Technology under the project code T2024-02-13.

#### REFERENCES

- [1] R. A. Buswell, W. R. Leal de Silva, S. Z. Jones, and J. Dirrenberger, "3D printing using concrete extrusion: A roadmap for research", *Cement and Concrete Research*, Vol. 112, pp. 37–49, 2018. <https://doi.org/10.1016/j.cemconres.2018.05.006>
- [2] M. A. Evans and R. I. Campbell, "A comparative evaluation of industrial design models produced using rapid prototyping and workshop-based fabrication techniques", *Rapid Prototyping Journal*, Vol. 9, pp. 344–351, 2003.
- [3] S. Lim, R. A. Buswell, P. J. Valentine, D. Piker, S. A. Austin, and X.D. Kestelie, "Modelling curved-layered printing paths for fabricating large-scale construction components", *Additive Manufacturing*, Vol. 12, pp. 216–230, 2016. <https://doi.org/10.1016/j.addma.2016.06.004>
- [4] L. Reiter, T. Wangler, N. Roussel, and R.J. Flatt, "The role of early age structural build-up in digital fabrication with concrete", *Cement and Concrete Research*, Vol. 112, pp. 86–95, 2018.
- [5] A.V. Rahul and M. Santhanam, "Evaluating the printability of concretes containing lightweight coarse aggregates", *Cement and Concrete Composites*, Vol. 109, 103570, 2020.
- [6] D. Marchon, S. Kawashima, H. Bessaies-Bey, S. Mantellato, and S. Ng, "Hydration and rheology control of concrete for digital fabrication: potential admixtures and cement chemistry", *Cement and Concrete Composites*, Vol. 112, 96–110, 2018.
- [7] F. Bos, R. Wolfs, Z. Ahmed, and T. Salet, "Additive manufacturing of concrete in construction: potentials and challenges of 3D concrete printing", *Virtual and Physical Prototyping*, Vol. 11, No. 3, pp. 209–225, 2016. <https://doi.org/10.1080/17452759.2016.1209867>
- [8] S. Alim Khan *et al.*, "The impact of nozzle diameter and printing speed on geopolymer-based 3D-Printed concrete structures: Numerical modeling and experimental validation", *Results in Engineering*, Volume 21, 101864, 2024.
- [9] Y. Wei *et al.*, "Numerical simulation of 3D concrete printing derived from printer head and printing process", *Journal of Building Engineering*, Volume 88, 109241, 2024.
- [10] L.i. Wang, Z. Tian, G. Ma, and M.o. Zhang, "Interlayer bonding improvement of 3D printed concrete with polymer modified mortar: experiments and molecular dynamics studies", *Cement and Concrete Composites*, Vol. 110, 103571, 2020.
- [11] D. Marchon, S. Kawashima, H. Bessaies Bey, S. Mantellato, and S. Ng, "Hydration and rheology control of concrete by admixtures for digital fabrication", *Cement and Concrete Research*, Volume 112, Pages 96-110, 2018.
- [12] R. Myrdal, "Accelerating admixtures for concrete - State of the art," Trondheim, 2007.
- [13] S. Muthukrishnan, S. Ramakrishnan, and J. Sanjayan, "Technologies for improving buildability in 3D concrete printing", *Cement and Concrete Composites*, Volume 122, 104144, 2021.
- [14] S. Kanagasantharam, S. Ramakrishnan, S. Muthukrishnan, and J. Sanjayan, "Effect of Magnetorheological additives on the buildability of 3D concrete printing", *Journal of Building Engineering*, Volume 74, 106814, 2023.
- [15] C. Zhang, V.N. Nerella, A. Krishna, S. Wang, Y. Zhang, V. Mechtcherine, and N. Banthia, "Mix design concepts for 3D printable concrete: A review", *Cement and Concrete Composites*, Vol. 122, 104155, 2021.
- [16] D. Marchon, S. Kawashima, H. Bessaies-Bey, S. Mantellato, and S. Ng, "Hydration and rheology control of concrete for digital fabrication: potential admixtures and cement chemistry", *Cement and Concrete Research*, Vol. 112, 96–110, 2018.
- [17] Packaged Dry, Hydraulic-Cement Grout (Nonshrink), TCVN 9204:2012, 2012.
- [18] Mortar for masonry - Test methods, Part 11: Determination of flexural and compressive strength of hardened mortars, TCVN 3121: 2022, 2022.
- [19] Cements - Test methods - Determination of setting time and soundness, TCVN 6017:2015, 2015.
- [20] D.J. Hannant, 4.11 – cement-based composites. In: Kelly A and Zweben C, *Comprehensive composite materials*, Oxford, UK: Pergamon, pp.323–362, 2000.
- [21] H. P. Nam, N. T. T. An, and D. T. Phuong, *Chapter 3: Composite construction materials, General construction materials*, Construction Publishing House, pp. 40–4, 2016.